Biochemical and Biophysical Research Communications 450 (2014) 318–323

Contents lists available at ScienceDirect

Biochemical and Biophysical Research Communications

journal homepage: www.elsevier.com/locate/ybbrc

Ablation of *Elovl6* protects pancreatic islets from high-fat diet-induced impairment of insulin secretion

Nie Tang [a], Takashi Matsuzaka [a,*], Marii Suzuki [a], Yuta Nakano [a], Hui Zao [a], Tomotaka Yokoo [b], Noriko Suzuki-Kemuriyama [a], Motoko Kuba [a], Yuka Okajima [a], Yoshinori Takeuchi [a], Kazuto Kobayashi [a], Hitoshi Iwasaki [a], Shigeru Yatoh [a], Akimitsu Takahashi [a], Hiroaki Suzuki [a], Hirohito Sone [c], Masako Shimada [a], Yoshimi Nakagawa [a], Naoya Yahagi [a], Nobuhiro Yamada [a], Hitoshi Shimano [a]

[a] Department of Internal Medicine (Endocrinology and Metabolism), Faculty of Medicine, University of Tsukuba, 1-1-1 Tennodai, Tsukuba, Ibaraki 305-8575, Japan
[b] Experimental Animal Laboratory, Research Center for Genomic Medicine, Saitama Medical University, 1397-1 Yamane, Hidaka City, Saitama 350-1241, Japan
[c] Department of Internal Medicine, Faculty of Medicine, Niigata University, 1-754 Asahimachi, Niigata, Niigata 951-8510, Japan

ARTICLE INFO

Article history:
Received 20 May 2014
Available online 2 June 2014

Keywords:
Fatty acid
Obesity
Type 2 diabetes
Insulin
Islet
β-cell

ABSTRACT

ELOVL family member 6, elongation of very long-chain fatty acids (Elovl6) is a microsomal enzyme that regulates the elongation of C12–16 saturated and monounsaturated fatty acids and is related to the development of obesity-induced insulin resistance via the modification of the fatty acid composition. In this study, we investigated the role of systemic Elovl6 in the pancreatic islet and β-cell function. Elovl6 is expressed in both islets and β-cell lines. In mice fed with chow, islets of the *Elovl6*$^{-/-}$ mice displayed normal architecture and β-cell mass compared with those of the wild-type mice. However, when fed a high-fat, high-sucrose (HFHS) diet, the islet hypertrophy in response to insulin resistance observed in normal mice was attenuated and glucose-stimulated insulin secretion (GSIS) increased in the islets of *Elovl6*$^{-/-}$ mice compared with those of the wild-type mice. Enhanced GSIS in the HFHS *Elovl6*$^{-/-}$ islets was associated with an increased ATP/ADP ratio and the suppression of ATF-3 expression. Our findings suggest that Elovl6 could be involved in insulin secretory capacity per β-cell and diabetes.

1. Introduction

Obesity is a major cause of type 2 diabetes (T2D) in humans because it leads to progressive deterioration of the insulin secretory function of the pancreatic β-cells and a reduced capacity to compensate for increased peripheral insulin resistance [1,2]. The accumulation of lipids in non-adipose tissues has been implicated in both pathologies, a phenomenon known as lipotoxicity as a molecular link between obesity and glucose homeostasis dysregulation [3,4]. Pancreatic β-cells are known to be highly susceptible to lipotoxicity, and both exogenous and endogenous sources of fatty acids (FAs) are believed to be involved in the deterioration of β-cell function.

The FA composition of lipid species could be another determinant of the development of lipotoxicity. ELOVL family member 6, elongation of very long-chain fatty acids (Elovl6) is a microsomal enzyme involved in the elongation of saturated and monounsaturated FAs with 12, 14, and 16 carbons [5,6]. Loss of Elovl6 function reduces stearate (C18:0) and oleate (C18:1n-9) levels and increases palmitate (C16:0) and palmitoleate (C16:1n-7) levels [7]. In our previous study, we reported that mice with the targeted disruption of Elovl6 (*Elovl6*$^{-/-}$) were protected against the development of hepatic insulin resistance when fed a high-fat, high-sucrose (HFHS) diet, despite similar degree of hepatosteatosis and obesity in these and the wild-type (WT) mice. Our findings suggest that FA composition, particularly the conversion of C16:0 to C18:0 plays a vital role in insulin sensitivity rather than mere lipid accumulation [7]. Therefore, the inhibition of Elovl6 could be a potential therapeutic target in the treatment of T2D. A major unanswered question is whether the inhibition of this elongase will lead to reduced susceptibility to pancreatic β-cell failure. Here, we investigated whether Elovl6 participates in the regulation of insulin secretion and β-cell function.

2. Materials and methods

2.1. Animals

Homozygous *Elovl6*$^{-/-}$ mice and sex- and age-matched *Elovl6*$^{+/+}$ littermates were housed in a pathogen-free barrier facility with a 12 h light/12 h dark cycle. Mice were maintained on standard lab-

* Corresponding author. Fax: +81 29 863 2081.
E-mail address: t-matsuz@md.tsukuba.ac.jp (T. Matsuzaka).

http://dx.doi.org/10.1016/j.bbrc.2014.05.113
0006-291X/

oratory chow or an HFHS diet [7]. All animal husbandry and animal experiments were consistent with the University of Tsukuba's Regulation of Animal Experiments and were approved by the Animal Experiment Committee of University of Tsukuba.

2.2. Cell culture

Mouse insulinoma MIN6 cells and mouse hepatoma Hepa1c1c7 cells were cultured as described previously [7,8].

2.3. Isolation of pancreatic islets

The isolation of mouse pancreatic islets was performed according to the collagenase digestion method s described previously [9].

2.4. Analysis of insulin secretion, insulin content, and DNA content of islets

Isolated islets were incubated for 2 h in RPMI 1640 medium supplemented with 10% FBS, 100 U/ml penicillin, and 100 μg/ml streptomycin. Ten islets were then preincubated for 30 min in 2.8 mM glucose in 0.5% BSA Krebs–Ringer Bicarbonate HEPES (KRBH) buffer. Finally, they were incubated in 2.8 mM glucose, 20 mM glucose, or 2.8 mM glucose with 30 mM KCl in 0.5% BSA KRBH buffer for 30 min, and insulin secretion was analyzed using a mouse insulin ELISA kit (Shibayagi). Insulin secretion, insulin content, and DNA content of the islets were measured as previously described [10].

2.5. Measurement of the ATP and ADP content of islets

ATP and ADP levels per 10 isolated islets were measured as described previously, using the CellTiter-Glo Luminescent Cell Viability Assay (Promega) [10].

2.6. Measurement of the triglyceride (TG) content of islets

One hundred isolated islets were used for lipid extraction. TGs were measured by extracting lipids using the method of Folch et al. [11], followed by TG determination with the GPO-trinder kit (Sigma) [10].

2.7. FA composition of islets

Total lipid was extracted from isolated islets (400 islets/sample) according to Bligh–Dyer's procedure [12]. After saponification, the FAs in each sample were methyl-esterified and the relative abundance of each FA was quantified by gas chromatography as described previously [7].

2.8. Gene expression

Total RNA extraction was performed using the NucleoSpin RNA kit (Takara) according to the manufacturer's instructions. cDNA was synthesized with the PrimeScript RT Master kit (Takara) and real-time PCR analysis was performed using the SYBR Green Dye (GeneAce SYBR qPCR Mix α; Nippon Gene) with an ABI 7300 instrument (Applied Biosystems) as previously described [10]. mRNA levels were normalized to cyclophilin expression.

2.9. Histology and quantification of islet mass

Mice were euthanized, and the pancreases were excised, fixed in 10% neutral buffered formalin, embedded in paraffin, and stained with hematoxylin and eosin.

2.10. Statistics

Data are presented as means ± SEM. An unpaired Student's *t*-test was used to compare the difference between the two groups. A P value of <-0.05 was considered statistically significant.

3. Results

3.1. Elovl6 is expressed in the pancreatic islet and β-cell lines

Real-time PCR analysis revealed that Elovl6 mRNA was present in isolated mouse islets as well as in the MIN6 cells (Fig. 1A and B) at the level comparable to that in the brain, liver, and white adipose tissue (WAT), where we have reported Elovl6 to play a metabolic role, suggesting a role of Elovl6 also in β-cells [6,7].

3.2. Morphology of islets of the *Elovl6*$^{-/-}$ islets

Chronic hyperinsulinemia resulting from insulin resistance is associated with hyperplasia and hypertrophy of islets caused by the adaptive proliferation of β-cells to maintain the blood glucose level. To determine whether endogenous Elovl6 is involved in the regulation of β-cell function under conditions of obesity, the WT and *Elovl6*$^{-/-}$ mice were fed a standard chow or an HFHS diet for 12 weeks. Consistent with our previous report [7], this high calorie diet markedly increased body weight, plasma insulin, and plasma glucose in WT mice (Supplementary Table 1). *Elovl6*$^{-/-}$ mice on the HFHS diet showed a significant reduction in plasma insulin and plasma glucose, and slight reduction in body weight compared to the HFHS WT mice. The histology of pancreatic sections demonstrated that the chow *Elovl6*$^{-/-}$ islets displayed no apparent morphological abnormalities (Fig. 2A). The HFHS WT mice showed a marked increase in islet size, suggesting an adaptive enlargement of β-cell mass in response to insulin resistance (Fig. 2A). In contrast, islet hypertrophy was suppressed in the HFHS *Elovl6*$^{-/-}$ pancreas compared with that in the HFHS WT pancreas (Fig. 2A

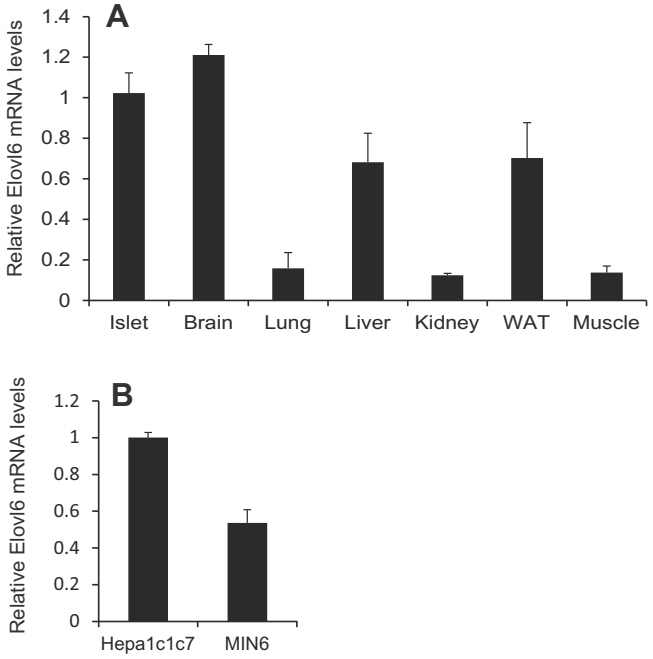

Fig. 1. Elovl6 is expressed in pancreatic islets and β-cells. (A) Elovl6 mRNA levels in the pancreatic islets and various tissues of 14–16-week-old male C57BL/6 J mice (n = 3). (B) Elovl6 mRNA levels in Hepa1c1c7 hepatoma cells and MIN6 cells (n = 4–5).

and B). This is presumably, at least in part, because Elovl6 deletion ameliorates the development of diet-induced insulin resistance [7]. Staining with antibodies against insulin and glucagon showed that the organization of β- and α-cells was preserved in the chow *Elovl6*$^{-/-}$ islet (Fig. 2C). The HFHS WT mice exhibited expanded β-cell mass and α-cell infiltration in islets, characteristic of β-cell dysfunction. However, α-cell infiltration was suppressed in the HFHS *Elovl6*$^{-/-}$ islets compared with that in the HFHS WT islets.

3.3. Glucose-stimulated insulin secretion (GSIS) is improved in islets isolated from *Elovl6*$^{-/-}$ mice

Insulin secretion was estimated from islets isolated from the WT and *Elovl6*$^{-/-}$ mice fed the chow or HFHS diet for 12 weeks (Fig. 3A). Basal insulin secretion in a low-glucose medium (2.8 mM) was similar between the WT and *Elovl6*$^{-/-}$ mice under both nutritional states. Insulin secretion in a high glucose medium (20 mM) evaluated on per cell-basis after DNA correction was slightly decreased in the HFHS WT islets compared with that in the chow WT islets. Conversely, the HFHS *Elovl6*$^{-/-}$ islets exhibited significantly higher insulin secretion than that in the chow *Elovl6*$^{-/-}$ islets and HFHS WT islets. Insulin secretion stimulated by KCl was slightly, but significantly, increased in the chow *Elovl6*$^{-/-}$ islets compared with that in the WT islets.

The insulin (Fig. 3B) and TG (Fig. 3C) contents of the *Elovl6*$^{-/-}$ islets were indistinguishable from those of the WT islets in the chow diet-fed mice, and these contents in islets increased in a similar manner in both the WT and *Elovl6*$^{-/-}$ islets in the HFHS diet-fed mice. Presumably explaining an enhanced GSIS, the ATP/ADP ratio of the HFHS *Elovl6*$^{-/-}$ islets was significantly increased compared with that of the HFHS WT islets (Fig. 3D).

3.4. Elovl6 deficiency alters islet FA composition

To estimate the impact of *Elovl6* deficiency on FA composition in pancreatic islets, we analyzed the FA composition of islets isolated from the WT and *Elovl6*$^{-/-}$ mice fed the chow or HFHS diet for 12 weeks (Fig. 4A). There were no significant differences in the C16:0, C16:1, C18:0, or C18:1 FA composition between the WT and *Elovl6*$^{-/-}$ mice fed the chow diet. However, the islet FA composition in the HFHS *Elovl6*$^{-/-}$ mice showed decreased C18:0 and increased C18:1 compared with that in the HFHS WT mice. The ratio of C18:0/C16:0, a marker of Elovl6 activity, was consistently decreased in the *Elovl6*$^{-/-}$ islets compared with that in the WT controls on both diets. The ratio of C18:1/C18:0, a marker of stearoyl-CoA desaturase-1 (SCD-1) activity, was increased in the islets of the HFHS *Elovl6*$^{-/-}$ islets compared with that in the HFHS WT islets.

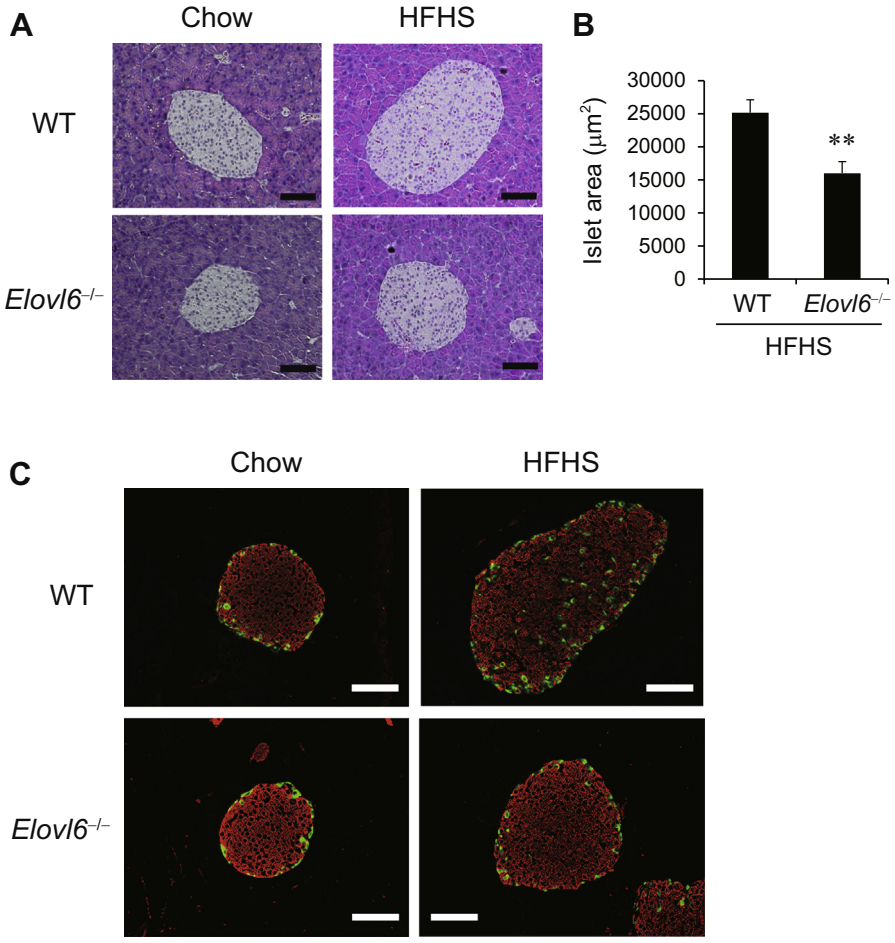

Fig. 2. Islet morphology of *Elovl6*$^{-/-}$ mice. (A) Representative pancreatic sections of wild-type (WT) and *Elovl6*$^{-/-}$ mice fed a chow or high-fat, high-sucrose (HFHS) diet for 12 weeks stained with hematoxylin and eosin for histological analysis. Scale bar, 50 μm. (B) Islet mass under the HFHS diet was quantified using NIH Image. At least 30 islets from each pancreas were quantified and the total number of islets scanned was 275–291 for each genotype ($n = 7$). $^{**}P < 0.01$. (C) Representative pancreatic sections of WT and *Elovl6*$^{-/-}$ mice fed a chow or HFHS diet, stained with insulin (red) and glucagon (green). Scale bar, 50 μm.

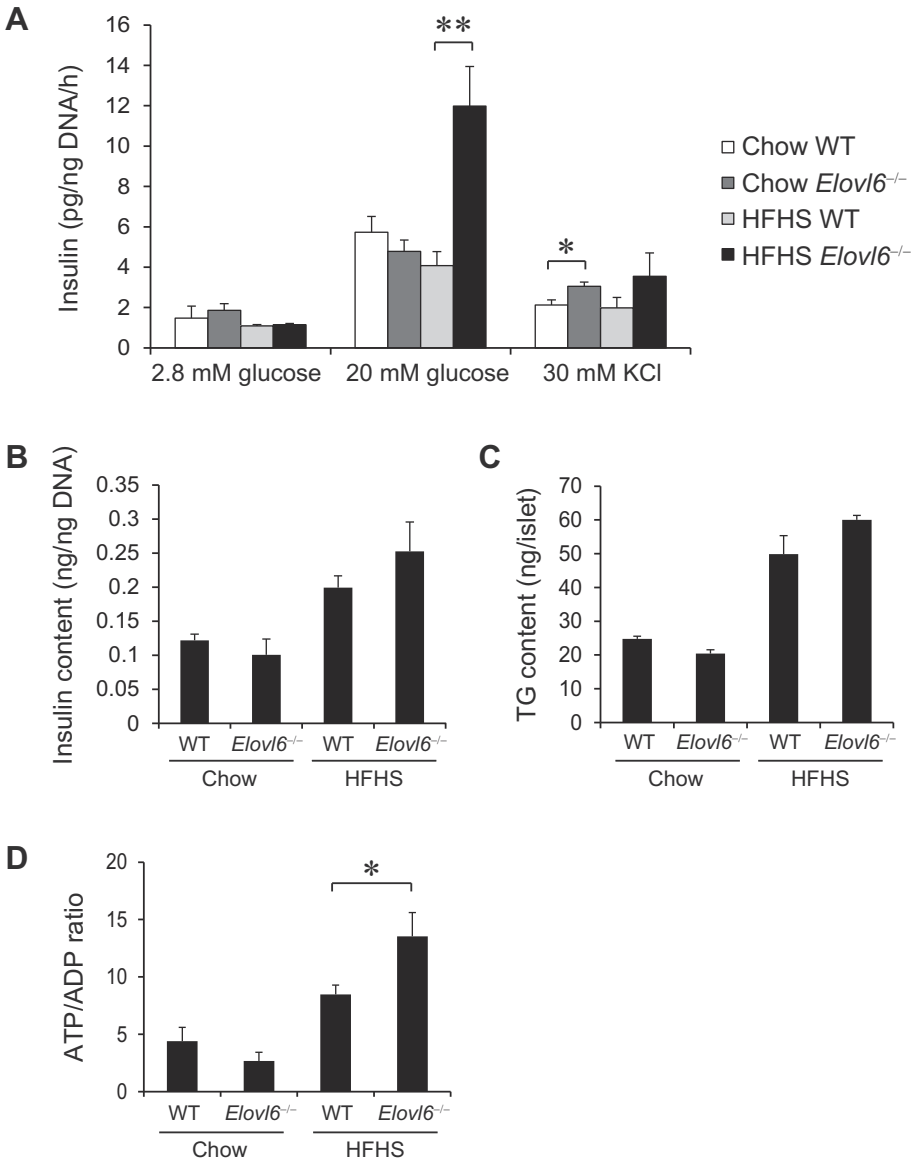

Fig. 3. Elovl6 deficiency results in enhanced islet glucose-stimulated insulin secretion and an increased ATP/ADP ratio. (A) Glucose- or KCl- stimulated insulin secretion from isolated islets of WT and *Elovl6*$^{-/-}$ mice fed a chow or high-fat, high-sucrose (HFHS) diet for 12 weeks ($n = 6$). (B) Insulin contents ($n = 4$), (C) triglyceride contents ($n = 4$), and (D) ATP/ADP ratio ($n = 5$–6) (D) in isolated islets of WT and *Elovl6*$^{-/-}$ mice fed a chow or HFHS diet for 12 weeks. $^{*}P < 0.05$, $^{**}P < 0.01$.

3.5. Sterol regulatory element binding protein-1c (SREBP-1c) and activating transcription factor-3 (ATF-3) are downregulated in the Elovl6$^{-/-}$ *islets*

Expressions of various genes in islets were estimated by real-time PCR to elucidate the molecular mechanism for enhanced insulin secretion in the HFHS *Elovl6*$^{-/-}$ islets. Expressions of lipogenic genes, including Elovl6 and SREBP-1c, were the same in the HFHS WT and chow WT mice, but those of fatty acid synthase (FAS) and SCD-1 were decreased in the former compared with the latter mice (Fig. 4B). Expressions of SREBP-1c and its target genes, FAS and SCD-1, were repressed in the chow *Elovl6*$^{-/-}$ islets compared with those in the chow WT islets. The expression of SREBP-1c was decreased, but that of FAS and SCD-1 was increased in the HFHS *Elovl6*$^{-/-}$ islets compared with that in the HFHS WT islets. The gene expression of uncoupling protein-2 (UCP-2), a SREBP target established to disrupt the β-cell energy metabolism and insulin secretion [13,14], was significantly increased in the HFHS WT islets, but not in the HFHS *Elovl6*$^{-/-}$ islets, explaining the increased ATP/ADP ratio in the latter mice (Fig. 4B). Expressions of pancreatic and duodenal homeobox factor-1 (PDX-1) and musculoaponeurotic fibrosarcoma oncogene family A (MafA), two master transcription factors regulating the insulin gene and GSIS in the mature β-cell [15], were decreased in the chow *Elovl6*$^{-/-}$ islets compared with those in the chow WT islets, but coordinately repressed by the HFHS diet in both groups (Fig. 4C). The expression levels of insulin receptor substrate-2 (IRS-2) and glucose transporter-2 (GLUT-2) were similar between the WT and *Elovl6*$^{-/-}$ mice (Fig. 4C). In the WT mice, the expression of ATF-3, the integrated stress response gene involved in β-cell dysfunction and apoptosis [16–20], was significantly increased with the HFHS diet (Fig. 4D). The HFHS *Elovl6*$^{-/-}$ mice displayed a markedly lower expression of ATF-3.

4. Discussion

In the present study, we showed that Elovl6 is significantly expressed in mouse islets and β-cell line MIN6 cells. Real

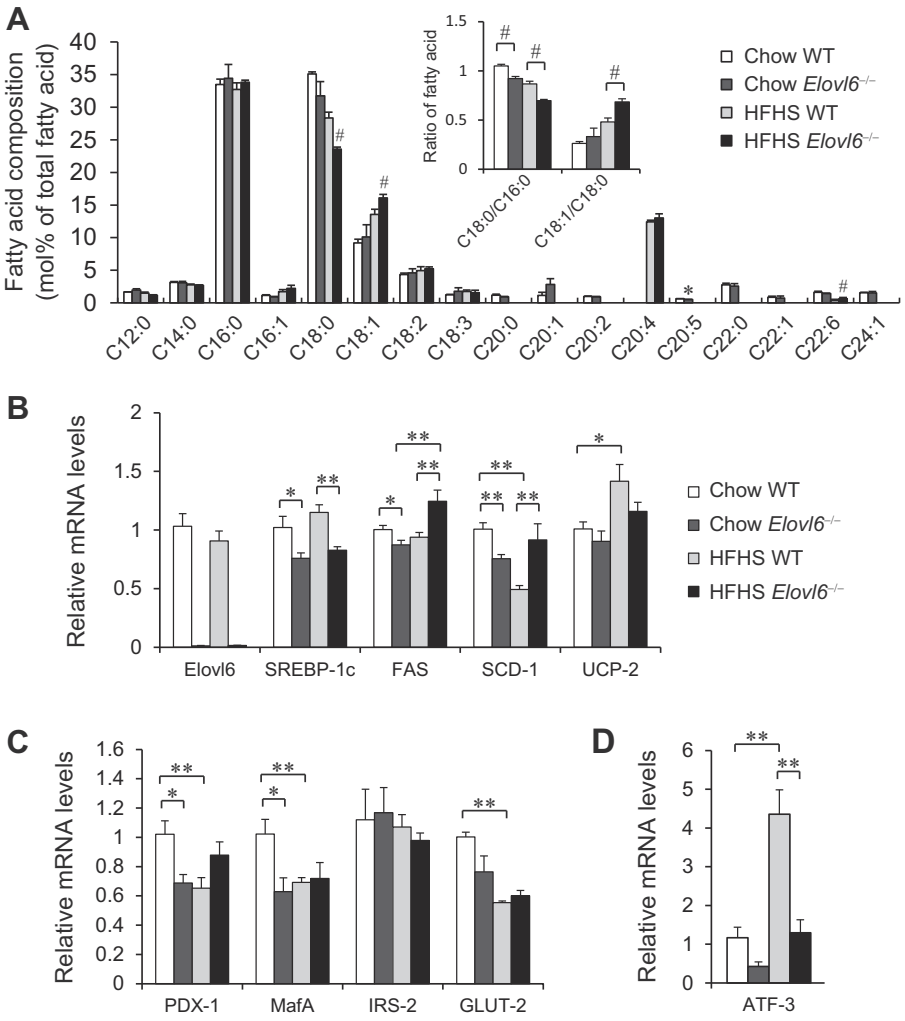

Fig. 4. Fatty Acid (FA) composition and gene expression profile in isolated islets from wild-type (WT) and *Elovl6*$^{-/-}$ mice fed a chow or high-fat, high-sucrose (HFHS) diet. (A) Islet FA composition of WT and *Elovl6*$^{-/-}$ mice fed a chow or HFHS diet for 12 weeks (n = 3–4). $^{*}P < 0.05$, $^{\#}P < 0.01$. (B) mRNA levels of genes involved in FA metabolism, (C) important for β-cell function, and (D) ATF3 in isolated islets from WT and *Elovl6*$^{-/-}$ mice fed a chow or HFHS diet for 12 weeks (n = 4–8). $^{*}P < 0.05$, $^{**}P < 0.01$.

time-PCR analysis revealed that Elovl6 is significantly expressed in the islet cells of the C57BL/6 J mice, and its expression in isolated islets is comparable to that in brain, liver, and WAT, where Elovl6 plays a regulatory role [6,7,21]. The chow *Elovl6*$^{-/-}$ mice did not show an altered islet morphology or β-/α-cell distribution, suggesting that Elovl6 is not required for the maintenance of islet architecture or β-cell mass in mice under normal conditions. However, the analysis of the expression of several genes related to FA metabolism and islet function revealed decreased levels in the chow *Elovl6*$^{-/-}$ islets. SREBP-1c, FAS, and SCD-1 contribute to FA synthesis [22], and PDX-1 and MafA contribute to β-cell-specific and glucose-responsive insulin gene transcription, suggesting that Elovl6 could play a role in islet function.

Our findings indicate that the *Elovl6*$^{-/-}$ mice resisted HFHS diet-induced islet hypertrophy, at least in part, as a result of enhanced insulin secretion capacity per cell. Meanwhile, as shown previously, the *Elovl6*$^{-/-}$ mice were protected from HFHS diet-induced hepatic insulin resistance [7]. In addition, IRS-2, reportedly important for the growth and survival of β-cells, was sustained in the *Elovl6*$^{-/-}$ islets. Thus, the attenuated β-cell expansion in the HFHS *Elovl6*$^{-/-}$ mice could be due to the combined effects of ameliorated insulin resistance and enhanced GSIS per β-cell.

Our results also indicate that the enhanced GSIS in the HFHS *Elovl6*$^{-/-}$ islets is not due to increased insulin content or reduced islet TG content but mediated through the elevation of the ATP/ADP ratio at high glucose concentrations. UCP-2, which regulate proton leak and has negative effects on ATP synthesis, was markedly upregulated in the HFHS WT islets, whereas it was increased only slightly in the HFHS *Elovl6*$^{-/-}$ islets, indicating that the improved glucose metabolism in β-cells partially contributed to the increment in GSIS.

One important aspect of this study is the potential effect of cellular FA composition on β-cell function. Our results show that the ratio of stearate in pancreatic islets is higher than that in other tissues such as liver, adipose tissue, and muscle. The relative amounts of C18:0 and the ratio of C18:0/C16:0 were significantly reduced by Elovl6 deficiency after the HFHS diet. Furthermore, the increase in the ratio of C18:1 to C18:0, which is consistent with the increased expression of SCD-1 in the HFHS *Elovl6*$^{-/-}$ islets, could prevent islets dysfunction caused by saturated FAs. Recently, Green et al. [23] clearly demonstrated that the knockdown of Elovl6 or overexpression of SCD-2 in INS-1 β-cells attenuated palmitate-induced endoplasmic reticulum (ER) stress and apoptosis. These results suggest that the FA composition of *Elovl6*$^{-/-}$ islets, namely the reduction of C18 FAs and the high ratio of C18:1/C18:0, may be protective against islet lipotoxicity in the HFHS diet-fed mice.

The suppression of ATF-3 expression in the HFHS *Elovl6*$^{-/-}$ islets could play an important role in the molecular mechanism

underlying enhanced GSIS. It has been demonstrated that ATF-3 is induced by signals relevant to pancreatic β-cell dysfunction such as proinflammatory cytokines, reactive oxygen species (ROS), ER stress, and high concentrations of glucose and FAs [16]. In addition, ATF-3 is involved in the reduction of PDX-1, which leads to pancreatic β-cell dysfunction and apoptosis [18]. Thus, the suppression of this factor could explain the improved β-cell function observed in the HFHS *Elovl6*$^{-/-}$ mice, although the molecular link between Elovl6 and ATF-3 remains unclear.

The phenotypes observed in the *Elovl6*$^{-/-}$ mice leave the question of the role of Elovl6 in β-cells unanswered. In the present study, it was not possible to distinguish in which islet cell type Elovl6 contributed to the phenotypes. Because a deficiency of Elovl6 causes a number of changes related to the phenotype of liver or other tissues [7,24–26], pancreatic β-cell-specific deletion will be required to further determine the precise role of Elovl6 in pancreatic β-cells.

In conclusion, our results show that Elovl6 is expressed in pancreatic islet and β-cells and that an Elovl6 deficiency inhibits impaired GSIS in obese mice. These findings suggest that this FA elongase may be involved in the regulation of islet function and open promising new perspectives for the prevention of T2D.

Acknowledgments

The authors thank Chizuko Fukui, Katsuko Okubo, and Yuko Tamai for their technical assistance, and Enago (www.enago.jp) for the English language review. This work was supported by the Japan Foundation for Applied Enzymology (to T.M.) and Grant-in-Aid for Scientific Research 24390230 (to H.S.) from the Ministry of Science, Education, Culture, and Technology of Japan.

Appendix A. Supplementary data

Supplementary data associated with this article can be found, in the online version, at http://dx.doi.org/10.1016/j.bbrc.2014.05.113.

References

[1] S.E. Kahn, R.L. Hull, K.M. Utzschneider, Mechanisms linking obesity to insulin resistance and type 2 diabetes, Nature 444 (2006) 840–846.
[2] C. Talchai, H.V. Lin, T. Kitamura, et al., Genetic and biochemical pathways of beta-cell failure in type 2 diabetes, Diabetes Obes. Metab. 11 (Suppl. 4) (2009) 38–45.
[3] R.H. Unger, Lipotoxicity in the pathogenesis of obesity-dependent NIDDM. Genetic and clinical implications, Diabetes 44 (1995) 863–870.
[4] N.A. van Herpen, V.B. Schrauwen-Hinderling, Lipid accumulation in non-adipose tissue and lipotoxicity, Physiol. Behav. 94 (2008) 231–241.
[5] Y.A. Moon, N.A. Shah, S. Mohapatra, et al., Identification of a mammalian long chain fatty acyl elongase regulated by sterol regulatory element-binding proteins, J. Biol. Chem. 276 (2001) 45358–45366.
[6] T. Matsuzaka, H. Shimano, N. Yahagi, et al., Cloning and characterization of a mammalian fatty acyl-CoA elongase as a lipogenic enzyme regulated by SREBPs, J. Lipid Res. 43 (2002) 911–920.
[7] T. Matsuzaka, H. Shimano, N. Yahagi, et al., Crucial role of a long-chain fatty acid elongase, Elovl6, in obesity-induced insulin resistance, Nat. Med. 13 (2007) 1193–1202.
[8] M. Ishikawa, F. Okajima, N. Inoue, et al., Distinct effects of pravastatin, atorvastatin, and simvastatin on insulin secretion from a beta-cell line, MIN6 cells, J. Atheroscler. Thromb. 13 (2006) 329–335.
[9] T. Kato, H. Shimano, T. Yamamoto, et al., Granuphilin is activated by SREBP-1c and involved in impaired insulin secretion in diabetic mice, Cell Metab. 4 (2006) 143–154.
[10] M. Ishikawa, Y. Iwasaki, S. Yatoh, et al., Cholesterol accumulation and diabetes in pancreatic beta-cell-specific SREBP-2 transgenic mice. a new model for lipotoxicity, J. Lipid Res. 49 (2008) 2524–2534.
[11] J. Folch, M. Lees, G.H. Sloane, Stanley, A simple method for the isolation and purification of total lipides from animal tissues, J. Biol. Chem. 226 (1957) 497–509.
[12] E.G. Bligh, W.J. Dyer, A rapid method of total lipid extraction and purification, Can. J. Biochem. Physiol. 37 (1959) 911–917.
[13] T. Yamashita, K. Eto, Y. Okazaki, et al., Role of uncoupling protein-2 up-regulation and triglyceride accumulation in impaired glucose-stimulated insulin secretion in a beta-cell lipotoxicity model overexpressing sterol regulatory element-binding protein-1c, Endocrinology 145 (2004) 3566–3577.
[14] A. Takahashi, K. Motomura, T. Kato, et al., Transgenic mice overexpressing nuclear SREBP-1c in pancreatic beta-cells, Diabetes 54 (2005) 492–499.
[15] H. Kaneto, T. Miyatsuka, D. Kawamori, et al., PDX-1 and MafA play a crucial role in pancreatic beta-cell differentiation and maintenance of mature beta-cell function, Endocr. J. 55 (2008) 235–252.
[16] M.G. Hartman, D. Lu, M.L. Kim, et al., Role for activating transcription factor 3 in stress-induced beta-cell apoptosis, Mol. Cell. Biol. 24 (2004) 5721–5732.
[17] D. Li, X. Yin, E.J. Zmuda, et al., The repression of IRS2 gene by ATF3, a stress-inducible gene, contributes to pancreatic beta-cell apoptosis, Diabetes 57 (2008) 635–644.
[18] W.H. Kim, M.K. Jang, C.H. Kim, et al., ATF3 inhibits PDX-1-stimulated transactivation, Biochem. Biophys. Res. Commun. 414 (2011) 681–687.
[19] J. Duprez, J.C. Jonas, Role of activating transcription factor 3 in low glucose- and thapsigargin-induced apoptosis in cultured mouse islets, Biochem. Biophys. Res. Commun. 415 (2011) 294–299.
[20] J.Y. Kim, K.J. Park, G.H. Kim, et al., In vivo activating transcription factor 3 silencing ameliorates the AMPK compensatory effects for ER stress-mediated beta-cell dysfunction during the progression of type-2 diabetes, Cell. Signal. 25 (2013) 2348–2361.
[21] H. Shimano, Novel qualitative aspects of tissue fatty acids related to metabolic regulation: lessons from Elovl6 knockout, Prog. Lipid Res. 51 (2012) 267–271.
[22] H. Shimano, Sterol regulatory element-binding proteins (SREBPs): transcriptional regulators of lipid synthetic genes, Prog. Lipid Res. 40 (2001) 439–452.
[23] C.D. Green, L.K. Olson, Modulation of palmitate-induced endoplasmic reticulum stress and apoptosis in pancreatic beta-cells by stearoyl-CoA desaturase and Elovl6, Am. J. Physiol. Endocrinol. Metab. 300 (2011) E640–E649.
[24] R. Saito, T. Matsuzaka, T. Karasawa, et al., Macrophage Elovl6 deficiency ameliorates foam cell formation and reduces atherosclerosis in low-density lipoprotein receptor-deficient mice, Arterioscler. Thromb. Vasc. Biol. 31 (2011) 1973–1979.
[25] T. Matsuzaka, A. Atsumi, R. Matsumori, et al., Elovl6 promotes nonalcoholic steatohepatitis, Hepatology 56 (2012) 2199–2208.
[26] H. Sunaga, H. Matsui, M. Ueno, et al., Deranged fatty acid composition causes pulmonary fibrosis in Elovl6-deficient mice, Nat. Commun. 4 (2013) 2563.